



Calcium Dynamics and Water Transport in Salivary Acinar Cells

James Sneyd¹ · Elias Vera-Sigüenza¹ · John Rugis¹ · Nathan Pages¹ · David I. Yule²

Received: 30 September 2020 / Accepted: 25 November 2020 / Published online: 17 February 2021
© Society for Mathematical Biology 2021

Abstract

Saliva is secreted from the acinar cells of the salivary glands, using mechanisms that are similar to other types of water-transporting epithelial cells. Using a combination of theoretical and experimental techniques, over the past 20 years we have continually developed and modified a quantitative model of saliva secretion, and how it is controlled by the dynamics of intracellular calcium. However, over approximately the past 5 years there have been significant developments both in our understanding of the underlying mechanisms and in the way these mechanisms should best be modelled. Here, we review the traditional understanding of how saliva is secreted, and describe how our work has suggested important modifications to this traditional view. We end with a brief description of the most recent data from living animals and discuss how this is now contributing to yet another iteration of model construction and experimental investigation.

Keywords Saliva secretion · Calcium oscillations · Water transport · Mathematical modelling · Three-dimensional finite element computations

1 Introduction

Secretion of saliva from the major salivary glands provides both fluid that hydrates and lubricates the oral cavity and proteins that begin to digest food. In addition, factors are also present in saliva that protect the oral cavity and upper gastrointestinal tract from bacterial and fungal assault. Malfunction of the salivary glands resulting in a

✉ James Sneyd
sneyd@math.auckland.ac.nz

¹ Department of Mathematics, The University of Auckland, Level 2, Building 303, 38 Princes Street, Auckland, New Zealand

² School of Medicine and Dentistry, University of Rochester Medical Center, 601 Elmwood Ave, Box 711, Rochester, NY, USA

reduction in fluid flow (a condition called *xerostomia*) results in difficulty swallowing and chewing food, a marked increase in dental carries and susceptibility to oral candidiasis, and leads to a severe deterioration in the quality of life. Xerostomia is associated with the auto-immune disease, Sjögren's syndrome, and is also commonly seen after radiotherapy for head and neck cancers (Ship et al. 1991; Melvin 1991; Fox and Maruyama 1997; Daniels and Wu 2000).

The most important early studies of saliva secretion were those of Lundberg (1956, 1957a, b) who was the first to propose that the principal underlying mechanism was the transport of Cl^- through the cell. A specific qualitative model was proposed by Silva et al. (1977); it is these studies that have provided the foundation for practically all subsequent work, including ours.

For almost 20 years, our group has used a combination of experimental and theoretical approaches to study the mechanisms of saliva secretion (Sneyd et al. 2003; Gin et al. 2007; Palk et al. 2010, 2012), and in 2014 we wrote a review of our major results (Sneyd et al. 2014). However, so much has changed since that time that another review is not only timely, but necessary. In particular, it is slowly becoming clearer that the traditional understanding of how saliva secretion works is not entirely accurate. The broad outlines remain the same, but the details have changed significantly.

The study of saliva secretion is a (fairly small) part of a much larger body of work on water transport by epithelial cells (Diamond and Bossert 1967; Swanson 1977; Weinstein and Stephenson 1979, 1981b, a; Reuss 2002; Dawson 1992; Mathias and Wang 2005; Chara and Bruschi 2015). Water transport by epithelia is important in a number of body parts; the lung epithelium maintains a surface layer of water which is critical for mucociliary clearance (with sample models by Novotny and Jakobsson 1996b, a; Warren et al. 2009; Garcia et al. 2013; Sandefur et al. 2017; Wu et al. 2018), the gut epithelium absorbs water (sample models by Larsen et al. 2000; Larsen 2002), while water absorption is a crucial function of epithelial cells in the kidney (sample models by Weinstein 1994, 1999; Layton and Layton 2005a, b; Layton 2011a, b; Weinstein 2020). In a manner similar to salivary secretion, tear and sweat glands also secrete water. Each of these areas relies on underlying models of water transport, a field which remains controversial, with a number of competing theories that we shall not discuss here. The interested reader is referred to Hill (2008), an excellent and readable review of the pros and cons of five major theories of physiological water transport.

2 Saliva Secretion: The Traditional View

The traditional explanation of saliva secretion goes as follows (Foskett and Melvin 1989; Martinez 1990; Nauntofte 1992; Cook et al. 1994; Melvin 1999; Turner and Sugiya 2002; Melvin et al. 2005; Ambudkar 2012; Lee et al. 2012). In a salivary gland, there are two major types of cells; firstly, the acinar cells, which are arranged in groups like a bunch of grapes or a blackberry (hence the name, from the Latin *acinus*, meaning a berry) and, secondly, the duct cells. Primary saliva is produced by the acinar cells and is collected in the acinar lumen (analogous to the stem of a bunch of grapes) whence it flows through the ducts to the mouth, emerging as secondary saliva (usually just called saliva).

2.1 Production of Primary Saliva

A salivary gland acinar cell is a polarised epithelial cell; it has a basal surface which faces to the interstitium and an apical surface which faces to the acinar lumen. At rest, the entry of Na^+ , Cl^- and K^+ through a $\text{Na}^+/\text{K}^+/2\text{Cl}^-$ cotransporter (NKCC1) in the basal membrane is balanced by the exit of Cl^- through the apical membrane into the lumen, the exit of K^+ across the basal membrane through a number of different types of K^+ channels, and the removal of Na^+ by the Na^+/K^+ ATPase (NaK) which is ubiquitous in all cells. This achieves internal ionic balance, control of cell volume and a very low flow of water through the cell, driven by slight differences in osmolarity; the water comes in across the basal membrane and exits the cell across the apical membrane into the lumen.

At rest, most cells have a cytoplasmic $[\text{Cl}^-]$ that minimises the electrochemical potential of Cl^- from inside to out. Indeed, many models of cell volume control—for example, the classic model of Tosteson and Hoffman (1960), see Keener and Sneyd (2008) for an introduction to models of cell volume control—incorporate this as a fundamental assumption. However, secretory epithelial cells such as salivary gland acinar cells accumulate Cl^- to much higher concentrations; they do this by the combined action of the basal NKCC1 cotransporter and the basal $\text{HCO}_3^-/\text{Cl}^-$ exchangers (AE2 and AE4). The NKCC1 cotransporter flux is, in turn, maintained by the $[\text{Na}^+]$ gradient created by the NaK ATPase.

It follows that, at rest, a salivary acinar cell is primed for Cl^- release into the lumen and thus primed for water transport. However, flow at rest is kept small as the apical Cl^- channels are mostly closed, thus allowing for only a small Cl^- flux into the lumen.

Production of much greater quantities of primary saliva is initiated by extracellular hormones or neurotransmitter (such as acetylcholine or cholecystokinin) that bind to G-protein-coupled receptors on the basal membrane, stimulating the production of inositol trisphosphate and the subsequent release of Ca^{2+} from the endoplasmic reticulum (Berridge et al. 2000; Berridge 2009; Ambudkar 2012, 2014; Dupont et al. 2016). The increase in cytosolic $[\text{Ca}^{2+}]$ activates two ion channels in particular; in the apical membrane Ca^{2+} -activated Cl^- channels (ClCa) release Cl^- into the lumen and depolarise the apical membrane. At the same time, Ca^{2+} -activated K^+ channels (KCa) in the basal membrane repolarise the membrane, allowing for a continued flow of Cl^- from the cell into the lumen. Water follows by osmosis, while charge balance in the lumen is maintained by a paracellular Na^+ current through the tight junctions into the lumen. The primary saliva that collects in the lumen is thus high in Na^+ and Cl^- .

In summary, the underlying driving force for saliva secretion is the transport of Cl^- from the interstitium, through the acinar cell, into the lumen. This sets up small osmotic gradients down which water flows from the interstitium, into the cell, and thence into the lumen. This is illustrated in Fig. 1.

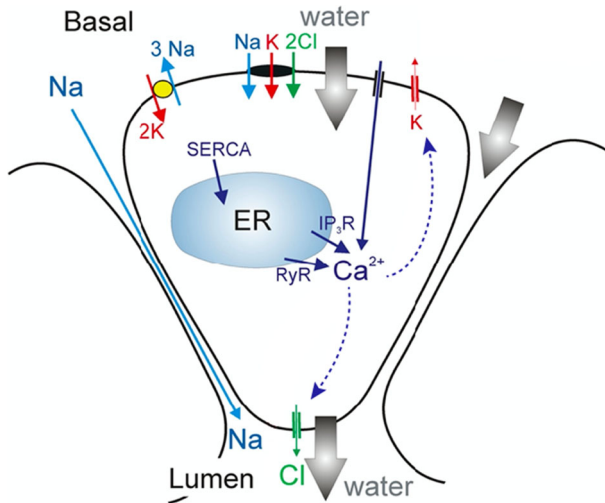


Fig. 1 Traditional view of saliva production (Melvin et al. 2005; Lee et al. 2012). At rest, uptake of Cl^- by a NKCC1 cotransporter maintains a high intracellular $[\text{Cl}^-]$. Agonist stimulation results in the release of Ca^{2+} from the endoplasmic reticulum (ER) through inositol trisphosphate receptors (IP_3R) and (possibly) ryanodine receptors (RyR). Calcium is re-sequestered into the ER by ATPase Ca^{2+} pumps (SERCA). Ca^{2+} activates Cl^- channels on the apical membrane and K^+ channels on the basal membrane (with possibly some on the apical membrane also). This results in the flow of Cl^- into the lumen, whereupon water follows by osmosis. Hence, in summary, Cl^- transport across the cell provides an osmotic gradient down which water flows, from the interstitium, through the cell, into the lumen. Charge balance is maintained by a paracellular Na^+ current

2.2 The Role of Ducts

As the primary saliva flows through the ducts, its ionic composition is changed by the duct cells that line the duct. Primary saliva has a high $[\text{Na}^+]$ and $[\text{Cl}^-]$ but a low $[\text{K}^+]$ and $[\text{HCO}_3^-]$ content. The duct cells replace the Na^+ and Cl^- with K^+ and HCO_3^- , so that secondary saliva has a high $[\text{K}^+]$ and $[\text{HCO}_3^-]$ but low $[\text{Na}^+]$ and $[\text{Cl}^-]$. However, the duct cells are impermeable to water.

Ionic balance is not at steady state by the time the saliva emerges into the mouth. We know this because the ionic composition of the secondary saliva depends on the rate of saliva secretion, with higher rates of secretion causing a decrease in $[\text{K}^+]$, and an increase in $[\text{Na}^+]$ in the secondary saliva (Mangos et al. 1973a, b).

2.3 Calcium Dynamics

Because saliva secretion is initiated by a rise in cytosolic $[\text{Ca}^{2+}]$, it is important to understand in detail the mechanisms that control $[\text{Ca}^{2+}]$, mechanisms that are common to almost all cell types. At steady state, the cytosolic $[\text{Ca}^{2+}]$ is low; Ca^{2+} influx into the cytoplasm is tightly controlled, while ATPase Ca^{2+} pumps (SERCA pumps) actively pump Ca^{2+} from the cytoplasm into the endoplasmic reticulum (ER), resulting in a resting $[\text{Ca}^{2+}]$ of around 50 nM, but a much higher $[\text{Ca}^{2+}]$ in the ER. Outside the

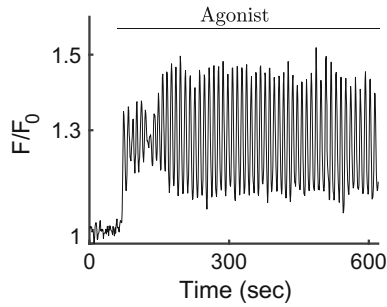


Fig. 2 Time series of the mean fluorescence of the Ca^{2+} indicator Fluo-4, averaged over a whole acinar cell in an intact mouse parotid gland (Pages et al. 2019). These oscillations were stimulated by the agonist carbachol, which binds to acetylcholine receptors. The fluorescence is closely related to $[\text{Ca}^{2+}]$, although the relationship is not linear. It is a good working assumption that the fluorescence is an analogue of $[\text{Ca}^{2+}]$, with oscillations with the same qualitative properties

cell, $[\text{Ca}^{2+}]$ is of the order of a few mM. In addition, the cytoplasm has many Ca^{2+} -binding proteins, or Ca^{2+} buffers, which contribute to the maintenance of a low resting cytosolic $[\text{Ca}^{2+}]$.

Hence, the cell cytoplasm is under enormous Ca^{2+} pressure. If Ca^{2+} channels in the cell membrane or the ER are opened, then Ca^{2+} will flow into the cytoplasm, quickly raising the cytosolic $[\text{Ca}^{2+}]$. Once these channels shut again, Ca^{2+} is removed from the cytoplasm by ATPase pumps, whereupon the influx channels reopen, leading to a second rise in $[\text{Ca}^{2+}]$. Repetition of this process results in repetitive spikes of increased $[\text{Ca}^{2+}]$, often called Ca^{2+} oscillations.

One particularly important concept for understanding (and modelling) Ca^{2+} oscillations is the idea of the *calcium toolbox*. There are many types of Ca^{2+} currents and fluxes that can let Ca^{2+} into the cytoplasm or remove it; these are the components of the toolbox. Membrane Ca^{2+} channels allow Ca^{2+} to flow from the interstitium into the cytoplasm, while ER Ca^{2+} channels (such as the inositol trisphosphate receptor, IPR, or the ryanodine receptor, RyR) allow Ca^{2+} to flow from the ER into the cytoplasm. Similarly, there are Ca^{2+} channels in other organelles such as the mitochondria and lysosomes. Ca^{2+} is removed from the cytoplasm by a range of different mechanisms, principally ATPases in the ER membrane and the cell membrane.

Each of the toolbox components has its own model, many of which can be found in Dupont et al. (2016). By using various combinations of these models, it is possible to construct a wide range of different models of Ca^{2+} oscillations, each adapted to a particular cell type.

The toolbox components also have well-defined spatial distributions, which are different for every cell type. By including these spatial distributions, it is possible to construct spatially distributed models tailored for different cell types. In this way, the study of Ca^{2+} dynamics combines limited variety with almost infinite flexibility. There are only a relatively small number of toolbox components, but they may be combined in essentially an infinite number of ways, leading to an endless variety of outcome.

Typical Ca^{2+} oscillations in an acinar cell from an intact mouse parotid gland are shown in Fig. 2. The overall shape is characteristic and seen in all responding cells in the gland, although the frequencies and amplitudes show considerable variety. The oscillations have a period of around 9 s, and are superimposed on a raised plateau.

2.4 Earlier Models

In our earlier work, we combined the above mechanisms into a unified spatially homogeneous model of saliva secretion, which was presented in detail in our previous review (Sneyd et al. 2014).

1. Agonist stimulation leads to the production of IP_3 which binds to IP_3 receptors (IPR) on the ER membrane, releasing Ca^{2+} from the ER into the cytosol. The IPR are restricted to the apical region (Kasai et al. 1993; Thorn et al. 1993; Thorn 1996; Nathanson et al. 1994; Lee et al. 1997), but IP_3 diffuses quickly through the cell. Hence, the IP_3 (which is produced at the basal membrane where the agonist receptors are located) is able quickly to activate the IPR at the other end of the cell.
2. Modulation of the production and degradation of IP_3 by Ca^{2+} leads to a feedback loop that results in an oscillation of cytosolic $[\text{Ca}^{2+}]$.
3. These Ca^{2+} oscillations activate Cl^- channels in the apical membrane and K^+ channels in the basal membrane. Cl^- flows into the lumen, while cytosolic Cl^- is maintained by the influx of Cl^- through the NKCC1 cotransporter in the basal membrane.
4. The osmotic gradient set up by these Cl^- fluxes drive the flow of water through the cell, from the interstitium to the lumen.

3 Recent Developments in Modelling Salivary Acinar Cells

Not surprisingly, the model as described above has had to be modified extensively as new experimental data have appeared, often in direct response to questions posed by the modelling.

3.1 Calcium Dynamics

One important parameter in the model is the exact spatial distribution of the IPR. It has been known for some years that the IPR are situated in the apical region of the acinar cell (Kasai et al. 1993; Thorn et al. 1993; Thorn 1996; Nathanson et al. 1994; Lee et al. 1997), but limited resolution in the data meant that it was only possible to say that the IPR were within approximately 200 nm of the apical ClCa channels. This supported the construction of models in which Ca^{2+} was able to modulate the rate of production and/or degradation of IP_3 , leading to positive or negative feedback that could result in oscillations. Such models are called Class II models (Dupont et al. 2016); we had already successfully tested predictions from a Class II model in a pancreatic acinar

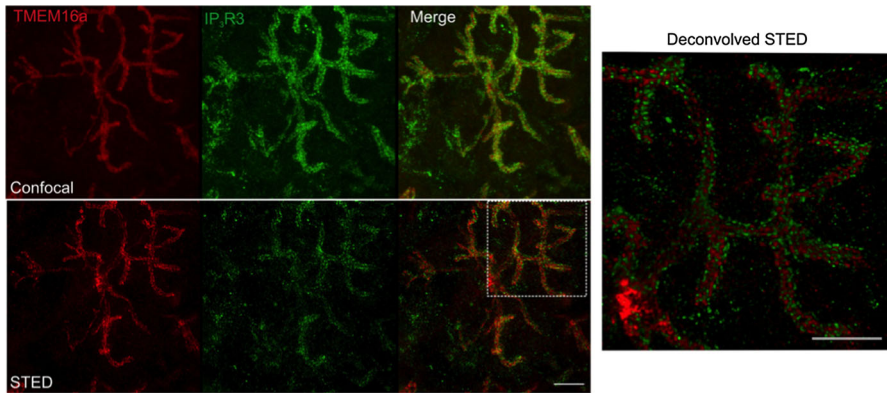


Fig. 3 Upper left panel: maximum projection of a confocal z stack (vertical resolution of $7\ \mu\text{m}$) showing CICa channels (TMEM16a) and type 3 IPR. The entire section was $80\ \mu\text{m}$ thick. Lower left panel: maximum projection of a stimulated emission depletion (STED) image. The STED image clearly shows that the proteins have distinct localisation. Right panel: Huygens deconvolution of the boxed region of the STED merged image. Scale bars = $5\ \mu\text{m}$

cell (Sneyd et al. 2006) which was additional motivation for using a Class II model for a parotid acinar cell, which is similar to a pancreatic acinar cell in many ways.

However, using Leica STED superresolution microscopy (Pages et al. 2019) we were able to show that the IPR and the CICa channels are nearly always located not further than $50\ \text{nm}$ from each other, and, furthermore, appear to be organised in puncta rather than being spread homogeneously through the apical region (Fig. 3). The spatial distribution of the IPR is critical, as they are the site of Ca^{2+} release. In a Class II model, the Ca^{2+} released from the IPR must be able to stimulate further production of IP_3 , which can occur only at the basolateral membrane (as this is where PLC is located). This means that the sites of Ca^{2+} release and IP_3 production cannot be too far apart. The old Class II model, which always struggled to cope with the requirement that the IPR were within $200\ \text{nm}$ of the apical membrane, was completely beaten by the new figure of $50\ \text{nm}$, and it became clear that our hypothesis for the mechanism underlying the Ca^{2+} oscillations was incorrect.

Our new model of Ca^{2+} oscillations in parotid acinar cells is a so-called Class I model, in which oscillations appear via modulation by Ca^{2+} of the IPR open probability (Dupont et al. 2016). Although in many Class I models this modulation takes the form of fast activation by Ca^{2+} followed by slower inactivation by Ca^{2+} , our latest IPR model (Cao et al. 2013; Sneyd et al. 2017) has a different mechanism. The IPR is still activated quickly by Ca^{2+} , but the inactivation of the IPR is now a result of the time-dependent rate at which the IPR responds to changes in $[\text{Ca}^{2+}]$. Although the overall behaviour is very similar to that of older Class I models, the underlying physiological assumptions are quite different.

With this new model, the apical region of the cell essentially turns into a pacemaking region. Ca^{2+} oscillations are generated, entirely within the apical region, by the interactions between Ca^{2+} and the IPR, and these oscillations are propagated as waves throughout the cell by a secondary excitable mechanism, based either on ryanodine

receptors or a different type of IPR (Pages et al. 2019). The Ca^{2+} oscillations in the apical region activate the CICa channels, while the propagated Ca^{2+} waves activate the basal KCa channels.

3.2 Chloride Reuptake

Another critical component of the saliva secretion mechanism is Cl^- reuptake. The Cl^- that is lost to the lumen across the apical membrane must be replenished by Cl^- entry across the basal membrane. Approximately 70% of this reuptake is accomplished by the NKCC1 cotransporter which brings in 1 Na^+ , 1 K^+ , and 2 Cl^- ions per cycle (Evans et al. 2000). However, the remaining 30% of Cl^- reuptake is HCO_3^- dependent, and involves two anion exchangers, AE2 (Slc4a2) and AE4 (Slc4a4) (Peña-Münzenmayer et al. 2015). Both AE2 and AE4 bring Cl^- into the cell and take HCO_3^- out, but AE4 anion transport is also linked to Na^+ exit.

The AE2 exchangers are paired with the NHE1 Na^+/H^+ exchangers, in a complex that allows for the control of intracellular pH, the removal of HCO_3^- and Na^+ , and reuptake of Cl^- .

Although both AE2 and AE4 are functionally expressed in salivary acinar cells and thus potentially involved in Cl^- reuptake, Peña-Münzenmayer et al. (2015) showed that, surprisingly, knockout of AE2 had no effect on saliva secretion, while knockout of AE4 decreased saliva secretion by approximately 35%. The most likely explanation for this discrepancy was the cotransport of Na^+ by the AE4, but it was not clear why such cotransport would make such a large difference.

This puzzle was explained, at least in part, by Vera-Sigüenza et al. (2018) who showed quantitatively how increased AE4 activity can compensate for the loss of AE2 activity. However, the loss of Na^+ transport when the AE4 are knocked out turns out to be critical; since the AE2 do not exchange Na^+ , they are unable to compensate for the loss of AE4 activity, and thus, Cl^- reuptake and saliva secretion are impaired upon AE4 knockout.

3.3 Potassium Channels and Pumping

In the traditional view of saliva secretion, KCa channels on the basolateral membrane are responsible for maintaining cell depolarisation during the efflux of Cl^- into the lumen. Since there is very little K^+ in primary saliva, it was thought that there could be few, if any, K^+ channels in the apical membrane, as otherwise it was thought that there would necessarily be significant levels of K^+ in the primary saliva. Furthermore, there was no evidence for the presence either of functional K^+ channels or NaK ATPases in the apical membrane.

This belief was challenged by Almássy et al. (2012) who used flash photolysis of caged Ca^{2+} to demonstrate the presence of functional KCa channels in the apical membrane of parotid acinar cells. Although modelling studies demonstrated that the presence of some K^+ channels in the apical membrane could increase the total amount of saliva produced (Palk et al. 2012), there remained no explanation of how this could result in primary saliva with very low $[\text{K}^+]$.

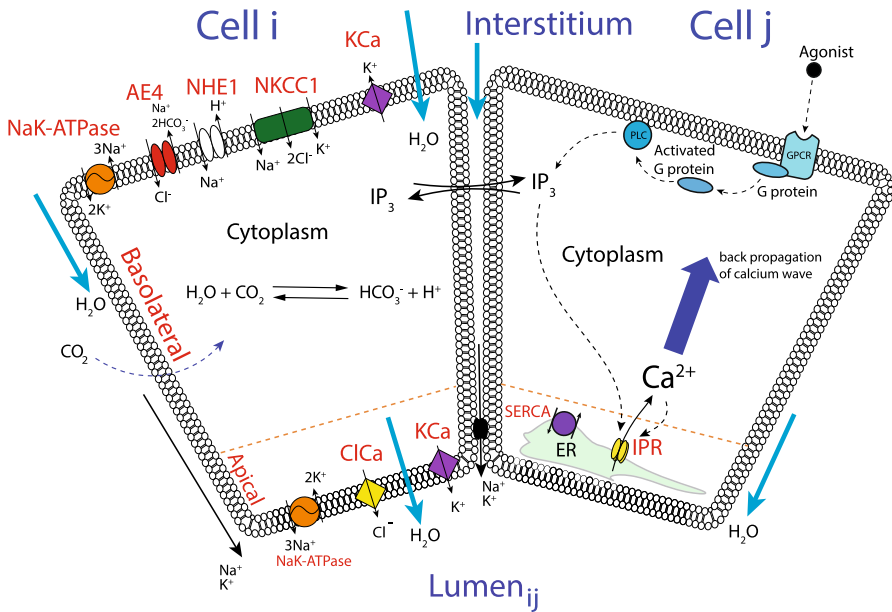


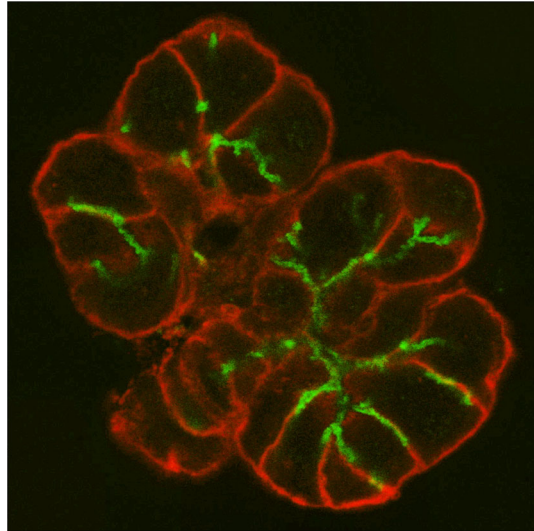
Fig. 4 New model of saliva secretion is similar in most respects to the traditional view discussed above, but with some important differences. Ca^{2+} is accumulated by the NKCC1 cotransporter and the AE4 anion exchanger, both of which are in the basal membrane. Upon agonist stimulation, IP_3 diffuses through the cell to the apical membrane where it binds to IPR located within 50 nm of the apical membrane. The apical region acts as a pacemaker, generating Ca^{2+} oscillations locally via Ca^{2+} modulations of the IPR open probability, and these oscillations are propagated across the cell by a secondary active mechanism, which could be either RyR or a different type of IPR. K^+ channels in the apical and basal regions maintain membrane depolarisation as Ca^{2+} flows into the lumen, and luminal $[\text{K}^+]$ is kept low by apical NaK ATPases

This discrepancy was partially resolved by Almásy et al. (2018) who showed that the apical membrane of parotid acinar cells contains both K^+ channels and NaK ATPase pumps, thus providing a mechanism for transport of K^+ into and out of the lumen. In the same paper, a mathematical model of this new mechanism showed how the luminal $[\text{K}^+]$ could be decreased approximately threefold by the NaK ATPase pumps in the apical membrane, while maintaining approximately 40% of the total cellular K^+ conductance in the apical membrane.

3.4 Summary of New Model

Our new model, incorporating the changes described above, is shown in Fig. 4. The major differences from the traditional model discussed above are, firstly, the presence of a substantial KCa current, as well as NaK ATPases, in the apical membrane, and, secondly, the tight clustering of the IPR with the apical ClCa channels.

Fig. 5 A typical frame from a z stack of confocal slices. The NaK ATPases are shown in red (giving the position of the basal membrane), while the apical CICa channels are shown in green (giving the position of the apical membranes). By stacking multiple such frames a three-dimensional picture of the group of cells, together with a branched lumen, can be reconstructed



4 Solving the Acinus Model

An important feature of our model was the construction of a three-dimensional finite element mesh upon which the model equations were to be solved. The mesh was based on z stacks of confocal slices with the apical and basal membranes labelled (Pages et al. 2019). The basal membranes were determined by labelling the NaK ATPase, while the apical membranes were determined by labelling the CICa channels.

A typical frame from the z stack is shown in Fig. 5, with the NaK ATPase shown in red and the CICa channels shown in green. Each membrane component can be traced (this was initially done manually) and then combined into a three-dimensional mesh. Each cell has well-defined apical and basal regions, and the boundaries between cells are conformal, in that the same set of boundary mesh points are in both the neighbouring cells. This allows for the computational solution of models with intercellular fluxes; thus, the model incorporates the intercellular diffusion of both Ca^{2+} and IP_3 , so that the cells are coupled.

The final grid (with an idealised lumenal structure) is shown in Fig. 6. In each cell, the apical region has a finger-like structure and sits between two different cells, while the overall structure of the lumen is similar to that of a tree. When considering this reconstruction it is important to keep in mind a number of things. Firstly, it is an idealisation only, based on a semi-manual reconstruction from the experimental z stack. Thus, one would necessarily expect there to be deviations from the structure of the actual cells. Secondly, the lumen is not a structure in its own right, it is instead simply a gap between cells. Here, the gap is drawn as a cylinder, but that is merely a simplification for the sake of clarity. In an alternative reconstruction the lumen has a varying width. Thirdly, important cell types, such as the myoepithelial cells and the duct cells, are entirely missing. Finally, the IPR are clustered within 50 nm at most of the apical membrane and thus display the same fingerlike structure as the lumen.

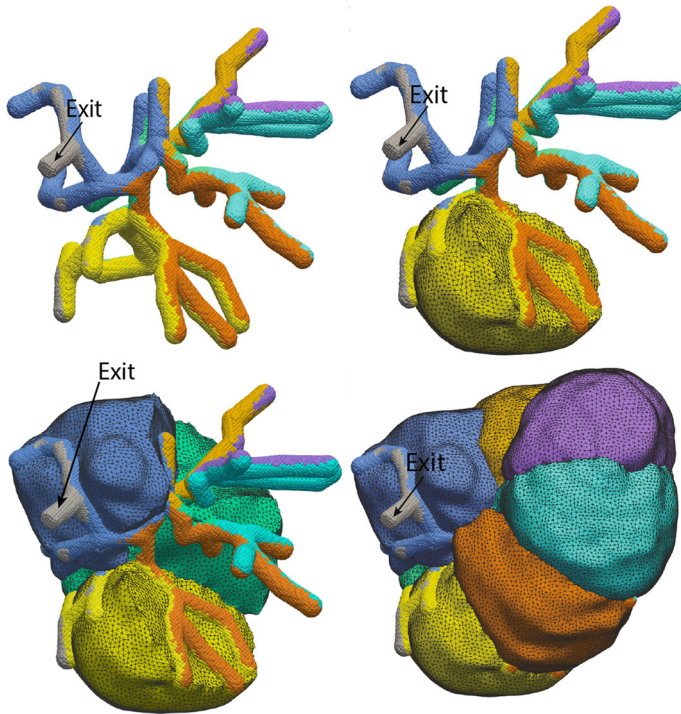


Fig. 6 Three-dimensional grid of seven acinar cells, together with an idealised reconstruction of the luminal structure. The lumen is colour-coded according to the colours of the cells that border each luminal segment. It is important to keep in mind that the lumen is not a stand-alone structure; it is simply the gaps between cells. The top left panel shows the isolated lumen; the top right panel shows how a single cell fits between the branches of the lumen; the bottom left panel shows how three cells fits in the luminal branches; the bottom right panel shows a view of all seven cells, with the lumen now almost entirely obscured

However, other receptors and channels are distributed uniformly over the appropriate membrane.

The model equations (given in full detail in Pages et al. 2019; Vera-Sigüenza et al. 2019, 2020) are solved on the 7-cell structure shown in Fig. 6. Ca^{2+} and IP_3 obey reaction–diffusion equations inside each cell and can move between cells at a rate that is proportional to the local concentration difference. All the cytosolic ions, with the exception of Ca^{2+} , are assumed to diffuse so fast that they can be treated as spatially homogeneous, but the apical and basal membrane potentials are modelled separately. Because of buffering, the effective diffusion coefficient of Ca^{2+} in the cytoplasm is low, allowing for significant intracellular $[\text{Ca}^{2+}]$ gradients. Fluid flow inside the lumen is highly simplified, being described simply by a total flow in response to changes in inflow and outflow. Pressure in the lumen is not included in the model.

The volume of the cell is computed also, and incorporated in the reaction–diffusion equations. However, our modelling of changes in volume is highly simplified; we do not recompute the mesh for each change in volume, we simply scale the diffusion coefficients and transport rates as needed. Since we have no information on how the

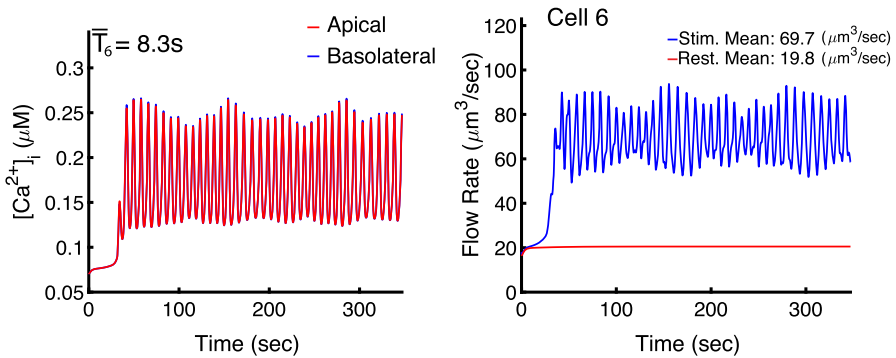


Fig. 7 Typical model results from cell 6 (Vera-Sigüenza et al. 2020). Results from the other cells are qualitatively similar. Left panel: time series of $[Ca^{2+}]_i$, spatially averaged over the apical and basal regions. At this resolution is it difficult to tell the difference between the apical and basal responses, but they are not identical. Right panel: the resting and stimulated rates of saliva secretion. Full details of the model output, including the apical and basal membrane potentials, and the cytoplasmic and luminal concentration of Na^+ , K^+ and Cl^- , can be found in Vera-Sigüenza et al. (2020)

shape of the acinar cell and the lumen changes as the cell shrinks, this is the simplest approach, requiring the fewest assumptions.

5 What Have We Learned from the Model?

Solution of the model equations gives Ca^{2+} responses and fluid flow that closely resemble data. A typical result (from cell 6) is shown in Fig. 7. In the apical region $[Ca^{2+}]_i$ oscillates with a period of about 8 s and each oscillation initiates a travelling wave of Ca^{2+} (not shown in the figure) which travels to the basal region, giving basal $[Ca^{2+}]_i$ oscillations with the same period and almost identical amplitude. The oscillations are superimposed on a raised baseline. Slight variations in amplitude are caused by intercellular coupling of nonidentical oscillators. Because each cell has a different shape and thus makes a different amount of IP_3 and has different numbers of IPR, each cell has a different oscillation period and amplitude. Since the cells are coupled by the intercellular diffusion of both IP_3 and Ca^{2+} (although the intercellular diffusion of Ca^{2+} has no discernible effect) these differences in oscillation period cause slight variations in the amplitude and period of the oscillations inside each cell, as expected from the general theory (Neu 1979; Ermentrout and Kopell 1984; Kopell and Ermentrout 1986, 1990; Mirollo and Strogatz 1990; Kuramoto 2003).

5.1 Oscillation Period is Unimportant

The usual theory of Ca^{2+} oscillations holds that the oscillations are a frequency-encoded signal; since a sustained rise in $[Ca^{2+}]_i$ is toxic to cells, the best way for a cell to use Ca^{2+} as an intracellular messenger is to carry the signal encoded in the frequency (Berridge and Galione 1988; Cuthbertson 1989; Berridge 1990; Thul et al.

2008; Dupont et al. 2011). There is considerable evidence from multiple cell types that this is indeed the case for many signalling pathways (Gu and Spitzer 1995; Dolmetsch et al. 1998; Li et al. 1998; Watt et al. 2000; Nash et al. 2002).

However, this does not appear to be the case for salivary acinar cells. The model predicts that, for a given average $[Ca^{2+}]$, the rate of saliva secretion is almost entirely independent of oscillation frequency (Vera-Sigüenza et al. 2020). Because it is difficult to measure accurately the water flow through a single cell, this prediction yet remains untested. However, the prediction is supported by preliminary intravital measurements (i.e. measurements in a living mouse, as discussed later) from mouse submandibular acinar cells which suggest strongly that the average $[Ca^{2+}]$ increases with increased stimulation, with little change in frequency. Thus, the rate of saliva secretion, which increases with increased stimulation, appears to depend on the average $[Ca^{2+}]$ rather than the Ca^{2+} oscillation frequency.

5.2 Do We Need a Multiscale Model?

Our multiscale model incorporates many known features of saliva secretion (particularly in the parotid gland), ranging from properties of the IPR measured at the single-channel level (Siekman et al. 2012; Cao et al. 2013) through to responses across multiple cells. It includes a range of membrane ion transport mechanisms that control intracellular ion concentrations and pH, and is based on an anatomical reconstruction so that the model is solved in a realistic domain.

Although these might seem like model advantages, this is not necessarily so. The full model is complex to program and takes a long time to run (a full run can take well over a day), which is potentially a serious problem. We wish to use the model to investigate how saliva secretion depends on a range of parameters, and to predict the outcome from a range of pathological situations. In addition, ideally we want to predict the fluid flow from an entire salivary gland, not just from the 7 cells chosen in this reconstruction. However, since it takes many hours to solve the model on only 7 cells, solving the model on 10,000 cells is not possible. Neither is it realistic to perform many hundreds of simulations, testing various parameter values and interventions.

On the other hand, we can have some faith in the predictions from this model. After all, predictions from a simple, but inaccurate model are easily obtained, but useless.

We attempt to resolve this conundrum by determining how far the full model can be simplified while still retaining the essential model behaviour. We emphasise that by “essential behaviour” we mean the total amount of fluid secreted by the group of cells. If a simplification of the model causes significant changes to the responses of individual cells, but no significant change to the average amount of fluid secreted by the acinus, then we claim that the essential behaviour is preserved by the simplification.

It turns out that the vast majority of the model complexity can be omitted without a significant change to the model predictions.

5.2.1 The Luminal Structure is Unimportant

We have previously shown that, in the limit as the membrane permeability to water gets large, and the osmotic gradient gets small, cells that are coupled by a common lumen act essentially as a single super-cell (Maclaren et al. 2012). In this case, the total amount of fluid secreted by N coupled cells is just the sum of the fluid secreted by each cell acting independently. Although this is theoretically true in the limit, it was unclear how accurate this would be in a more realistic situation. It turns out that, in our model, the membrane permeability to water is high enough, and the osmotic gradient is low enough, that this situation holds in most cases (Vera-Sigüenza et al. 2020). Simulations of a simplified version of the model, in which each cell is independent of the others (and not coupled via the common branching lumen shown in Fig. 6), show that total fluid flow (mostly) remains practically unchanged.

This result is not an artefact of our particular luminal topology. When the model is computed for an arbitrary selection of different luminal topologies (i.e. with the cells connected by a common lumen in a different way), the total fluid flow is the same in each case (Vera-Sigüenza et al. 2020), and in each case is equal to the flow that would be generated by 7 cells acting independently.

The exception to this general rule is for model cells that demonstrate spontaneous Ca^{2+} oscillations at rest. In the model this can happen when the cell is small, but this is an artefact of parameter selection, as we did not parameterise the model differently for every cell, thus avoiding any hint that our results depend on careful cell-dependent parameter selection. However, in an actual salivary gland we have not seen any evidence that any cells exhibit spontaneous Ca^{2+} oscillations at rest.

The reason for this exception is that, if an isolated cell has a spontaneous Ca^{2+} oscillation at rest (and thus significant fluid flow at rest), this oscillation can disappear when the cell is connected to others via a common lumen. In this case, the coupling via a common lumen has a significant effect on the resting fluid flow, although no significant effect on the fluid flow when all the cells are stimulated.

5.2.2 Spatial Structure and Intercellular Communication are Unimportant

If the internal spatial structure of each cell is ignored and the Ca^{2+} dynamics modelled with an ODE rather than a PDE, there is very little difference in total fluid flow. There are two slightly different ways of constructing an approximate ODE; firstly, one can simply model the cell as a homogeneous region, making no distinction between apical and basal regions, or, secondly, one can model the cell as two coupled spatially homogeneous regions, corresponding to the apical and basal regions. In either case, the total fluid flow of the acinus is almost unchanged (Vera-Sigüenza et al. 2020).

More surprising, perhaps, is the result that the intercellular diffusion of Ca^{2+} and IP_3 makes no significant difference to the total fluid flow. Intercellular diffusion of Ca^{2+} makes little difference to anything at all; this is because any Ca^{2+} that gets through a gap junction (which are assumed to be homogeneously distributed on the lateral surfaces of each cell) is quickly bound by Ca^{2+} buffers.

However, intercellular diffusion of IP_3 has a significant effect on the intracellular Ca^{2+} dynamics of each cell, particularly at low coupling strength. This is because each

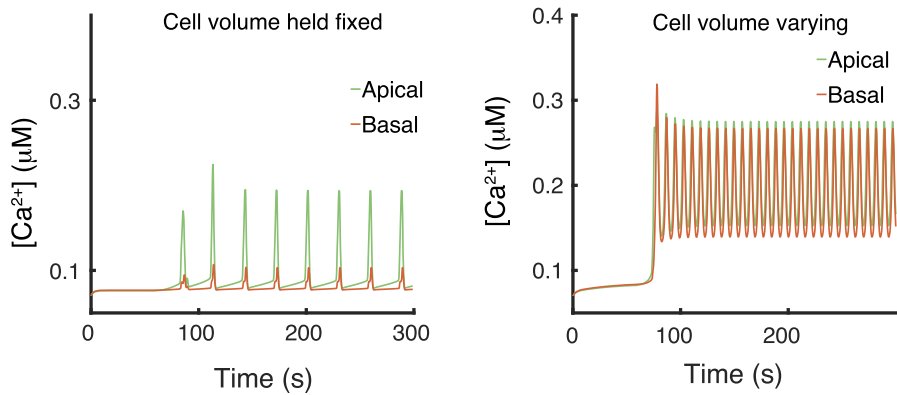


Fig. 8 Model oscillations from a single independent cell (Pages et al. 2019), showing the effect of incorporating changes in cell volume. If the volume of the cell is artificially held constant, the model oscillation is slower and not superimposed on a raised plateau. The concentrations are averaged over the apical and basal regions

cell is an autonomous oscillator with a period different to that of its neighbours. When non-identical oscillators are coupled, we know from the general theory that when the coupling strength is high the oscillators can synchronise, but when the coupling strength is lower (but not zero) much more complex behaviour can appear (Torre 1975).

Although this general result remains true in our model, the overall fluid flow simply doesn't care. The details of the oscillations in each cell might change, but the average $[Ca^{2+}]$ doesn't change greatly, and that is all that matters for the fluid flow. Thus, even at high intercellular coupling strength, when the individual cellular oscillators are significantly perturbed by their neighbours, total fluid flow remains unaffected. This is true for all stimulation levels.

5.3 The Change in Volume is Critical

As it transports water, each cell shrinks in volume by approximately 30% (Foskett and Melvin 1989), and this effect is incorporated into our model. Indeed, it's not possible to construct a model of water transport without taking the volume change into account. In our model, the change in volume is included both in the water transport equations and in the Ca^{2+} dynamics equations. Surprisingly, it turns out that the change in volume upon stimulation plays a significant role in the Ca^{2+} dynamics. When volume changes are not incorporated in the Ca^{2+} dynamics model, the Ca^{2+} oscillations have a much larger period and are not superimposed on a raised baseline (Fig. 8). However, incorporation of volume changes into the Ca^{2+} model changes the oscillations into the form seen experimentally.

It follows that the Ca^{2+} dynamics of a salivary acinar cell cannot be understood independently of an understanding of water transport; these two processes are inextricably linked.

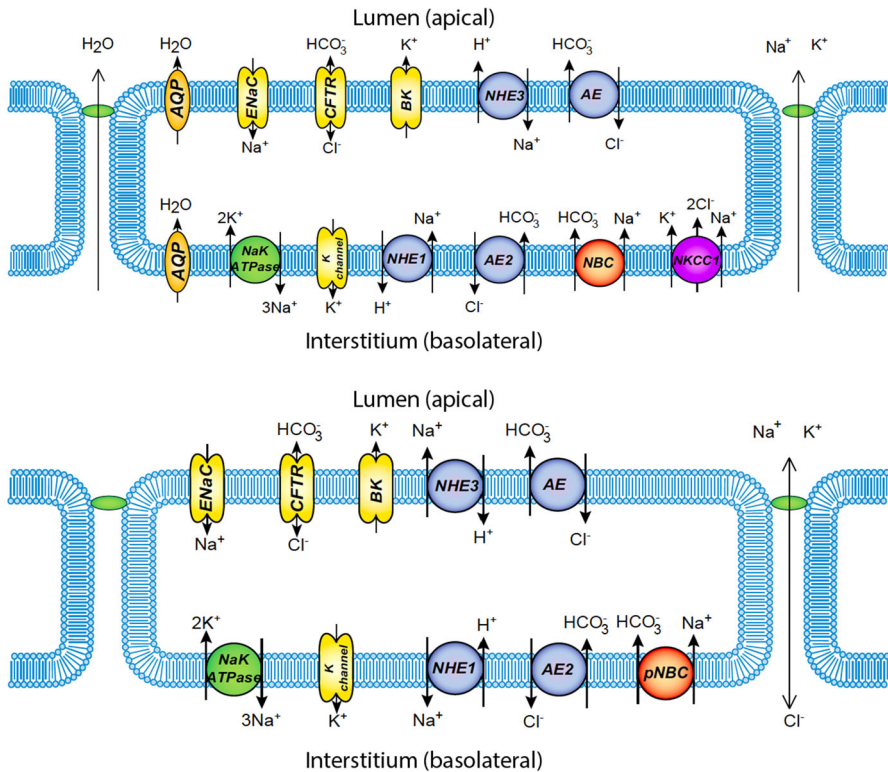


Fig. 9 Schematic diagrams of two different kinds of duct cells (Fong et al. 2017). The upper panel describes a duct cell that allows for transcellular and paracellular water transport, while the lower panel describes a duct cell that allows no water transport. ENaC is the epithelial Na^+ channel; CFTR is the cystic fibrosis transmembrane regulator anion channel that allows both Cl^- and HCO_3^- current; BK is the usual K^+ channel (i.e. not the Ca^{2+} -dependent version seen in acinar cells); NHE1 and NHE3 are Na^+/H^+ exchangers; NBC is a $\text{Na}^+/\text{HCO}_3^-$ cotransporter; K channel is a generic unspecified K^+ channel

6 Recent Developments in Modelling Salivary Duct Cells

Less is known about salivary duct cells than about salivary acinar cells. The traditional view of them is that they mostly just transport Na^+ and Cl^- out of the duct, and K^+ and HCO_3^- into the duct, while remaining impermeable to water. There are two major types of duct cells; intercalated duct cells, which are closer to the acinus, and striated duct cells, which are further downstream. There is evidence that intercalated duct cells transport water (Lee et al. 2012; Hong et al. 2014), although less than acinar cells do, but there remains general agreement that striated duct cells are impermeable to water.

The secondary saliva that flows out of the ducts and into the mouth is hypotonic to the interstitium, which explains why much of the duct must be impermeable to water. If it wasn't, then water would be drawn out of the duct by osmosis, leading to a decrease in saliva secretion.

Recent developments in gene therapy to treat xerostomia arising from irradiation for head and neck cancers have motivated a more detailed understanding of how duct cells work. Briefly, in the 1990s it was conjectured that transferral of the gene for the human hAQP1 aquaporin (water channel) to salivary ducts which had been damaged by irradiation might be able to restore salivary function, at least partially (Baum et al. 2006, 2010, 2017). This was first shown to work well in rats and minipigs, and around 2012 a clinical trial showed that this therapy would also work in humans (Gao et al. 2010; Baum et al. 2015).

However, given current understanding of how the ducts work, this outcome was rather a puzzle. It was thought that the aquaporins were mostly ending up in the duct cells, thus making them permeable to water, but it was not clear why this didn't result in water leaving the ducts, rather than entering them.

An initial model by Patterson et al. (2012) was later modified and extended by Fong et al. (2017) (Fig. 9), based largely on the qualitative model of Lee et al. (2012). They concluded that, firstly, the hAQP had to be transfected only into the intercalated duct cells, and that transfection of the gene also changed the expression of other ionic transport mechanisms. For example, the model predicted that, after transfection, the nonsecretory duct cells would have fewer ENaC and CFTR channels, but more apical NHE exchangers. These model predictions have not yet been tested, and neither have they been rigorously tested for robustness. Hence, it is fair to say that our current understanding of how ducts work, either before or after transfection, remains uncertain.

7 The Next Generation of Models

Most recently (in early 2020), exciting new data have appeared that threaten to overturn yet again our ideas of how salivary acinar cells work.

Developments in genetic manipulation and microscopy have now made it possible to measure, at high spatial and temporal resolution, Ca^{2+} responses in the submandibular gland of a living mouse, in response to direct neural stimulation. Since all previous results were from isolated cells or glands, and the responses were stimulated by direct application of agonist to the cells, this is the first time it has been possible to determine salivary gland Ca^{2+} responses in a realistic physiological setting.

Preliminary results are surprising in two particular ways.

1. It appears that, in response to neural stimulation ranging from 2 to 10Hz, the $[\text{Ca}^{2+}]$ in submandibular acinar cells oscillates with a period of around 1 s, much faster than the oscillations seen in isolated cells or glands (in response to direct application of agonist). These fast oscillations still occur on a raised baseline. Preliminary results are shown in Fig. 10.
2. The fast oscillations described above occur principally in the apical regions of the cell, and do not appear to be propagated to the basal regions to any significant extent. Preliminary results are shown in Fig. 11.

Clearly, these new data paint a very different picture than the older data from isolated cells and glands. The Ca^{2+} oscillations seem no longer to be periodic intracellular waves, being far more spatially restricted, and their frequency is much higher.

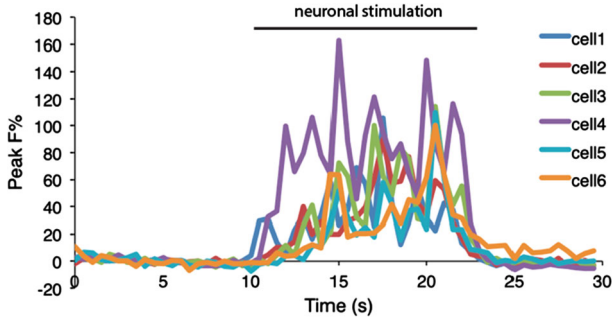


Fig. 10 Preliminary data from intravital measurements of Ca^{2+} oscillations in acinar cells from the submandibular gland acinar cell of a living mouse. (These data are a low-resolution version of more extensive high-resolution data that are submitted for publication.) The oscillations were initiated by neuronal stimulation, which results in the release of acetylcholine. Neuronal stimulation was 5 mA at 5 Hz, for 12 s, and responses were measured at 2 fps. The 6 cells are all from different acini. These intravital oscillations were stimulated by activation of the same receptor as those from an intact gland, as shown in Fig. 2, but their frequency is significantly higher

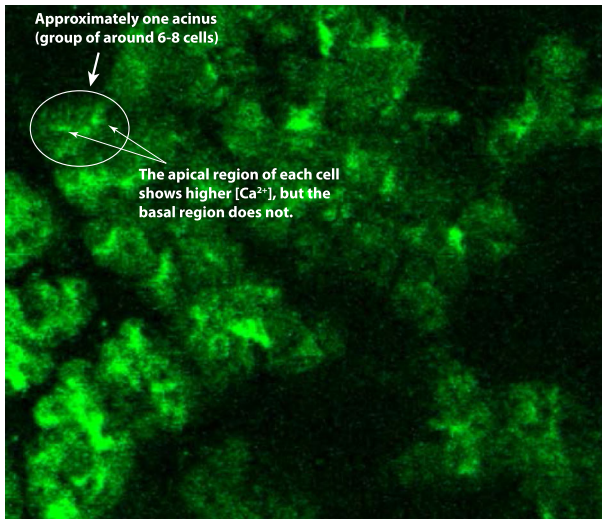


Fig. 11 A still image from a video of intravital Ca^{2+} oscillations in acinar cells from the submandibular gland of a living mouse, in response to neuronal stimulation. (These data are a low-resolution version of more extensive high-resolution data that are submitted for publication.) The majority of the cells demonstrate Ca^{2+} oscillations only in their apical regions

We must, of course, keep in mind that the new data are from the submandibular gland, not the parotid gland, and thus, it is possible that Ca^{2+} oscillations in parotid gland acinar cells (in living animals) are similar to those observed in isolated parotid acinar cells and glands. However, because of the extensive similarities between parotid and submandibular acinar cells, this is not the most plausible way to resolve the discrepancies between the old data and the new. It is more likely that the discrepancies

are caused by the fact that, in the living animal, the cells are stimulated directly by the nerves, as would occur physiologically.

7.1 The Proposed New Paradigm

It is particularly interesting that our new observations of Ca^{2+} signalling in submandibular acinar cells are consistent with previous work on the spatial positioning of the KCa channels and the NaK ATPase pumps.

As we discussed above, there is mounting evidence that the apical membrane of acinar cells contains KCa channels and NaK ATPase pumps, in addition to the ClCa channels. Our new intravital data suggest why this should be so. First, we note that, since the ClCa current moves the membrane potential towards the Nernst potential of Cl^- (in which case the Cl^- current would stop), the cell requires the activation of K^+ channels to counterbalance the Cl^- current. However, in the absence of a propagated Ca^{2+} wave across the cell, KCa channels can only be activated if they are in a region where the $[\text{Ca}^{2+}]$ increases, i.e. in the apical region. Thus, our new data suggest that the cell will secrete water properly only if the apical region has a substantial K^+ current. This apical K^+ current, rather than being a non-critical byproduct of the modelling studies, now appears to have morphed into a critical feature.

In addition, since we still know that the primary saliva is low in K^+ , the K^+ that flows into the lumen needs to be removed, and this appears to be the function of the apical NaK ATPase pumps.

Thus, all these results are converging to a new version of saliva secretion in salivary gland acinar cells, as illustrated in Fig. 12. In this new model the regulation of water transport occurs almost exclusively in the apical region; because of their spatial proximity, the Ca^{2+} released from the IPR has enhanced access to the two critical Ca^{2+} -dependent ion channels that control the membrane potential and the Cl^- current.

There is, as yet, no quantitative description of this proposed new model, so it remains unclear how well this new approach will deal with the harsh requirements of a stable cell volume and electroneutrality. Although it is also unclear whether or not our previous conclusions about the unimportance of the spatial structure of the acinar lumen will remain accurate, it is a reasonable first guess that they will. Finally, it is plausible that intracellular spatial variation of $[\text{Ca}^{2+}]$ will be even less relevant in a new model of an acinar cell; we thus anticipate that an ODE model of the apical region of the cell, coupled to the water transport mechanisms as before, will be an accurate and predictive model.

Many spatial questions remain, also. For example, what exactly is the spatial pattern of ACh released by neuronal stimulation? Is each acinus innervated equally, and does each acinar cell receive the same level of agonist stimulation? Does it matter if they do, or don't?

7.2 What About Duct Cells?

So far we have concentrated our attention on the next generation of models of the salivary acinar cells, simply because more is known about them. However, new data

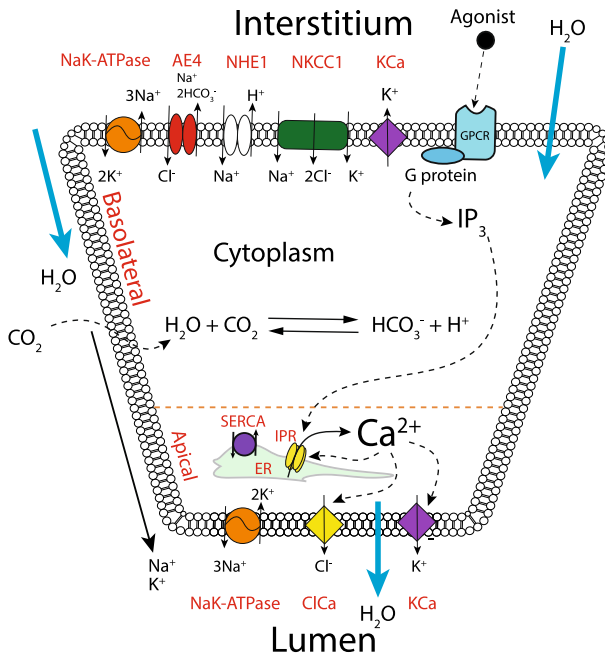


Fig. 12 A proposed new hypothesis for saliva secretion in salivary acinar cells. The only difference from the model shown in Fig. 4 is that there is now no Ca^{2+} wave propagated across the cell, from apical to basal, and thus, all the necessary Ca^{2+} -modulated ion channels now reside in the apical region. They can also exist in the basal membrane but do not need to be activated to a significant extent. No quantitative description of this proposed model yet exists

are beginning to appear from duct cells now also, again in the submandibular gland. These new data take time to collect as they rely on mouse genetic constructs which take time to breed and grow, but preliminary data are already good enough for us to be able to start the construction of three-dimensional models of acini and ducts together.

Given that one of our major conclusions is that the spatial structure of the lumen is not important, and given also that our new understanding of how an acinar cell works suggests that the intracellular structure is also unimportant, why would we bother at all with constructing three-dimensional models of a combined acinus and duct?

There are two principal answers to this question. Firstly, we still do not know if our previous conclusions will stand the test of the new model, based on our new data. Secondly, we also do not know how spatial structure affects the function of the duct. Although we might suspect it has little effect, we will not know for sure unless we test it.

On the other hand, our previous mesh construction methods were partially manual and very time-consuming; it would not seem to be a good use of time to continue with such slow (although accurate) approaches if our expectation is that the spatial structure will have little importance. We have thus developed a method for the fully-automated construction of a three-dimensional mesh of a combined acinus and duct with the correct spatial statistics on average, as determined from the data. Any particular mesh

will not be an accurate description of any particular group of cells, but it will have the correct average properties. This work remains ongoing.

One of the first questions to be addressed by this new generation of duct models is whether or not our predictions from the simplified model (Fong et al. 2017) of hAQP transfection remain valid in a more accurate model. In addition, the robustness of these predictions with respect to spatial structure needs to be assessed carefully.

8 Conclusions

Over the past 15 years or so, our combined theoretical/experimental work has taught us a great deal about how saliva secretion works, and we are on the verge of the next generation of results and models. Even more importantly, we are on the verge of discovering much more about how saliva secretion works in living animals, in response to physiological patterns of neuronal stimulation.

From the modelling point of view, one of our most important results has a rather negative flavour. We have strong evidence that a multiscale model is not necessary if the goal is to understand how much saliva is secreted. The Ca^{2+} dynamics in individual cells are dependent on a host of factors, including intercellular permeability to IP_3 , and the size and structure of the apical and basal regions. Nevertheless, it appears that each acinar cell simply averages out the $[\text{Ca}^{2+}]$ in the apical region of the cell, and pays almost no attention to the fine structure of the Ca^{2+} oscillations. The oscillation period, for example, plays no significant role in determining the rate of saliva secretion. In addition, the fine spatial structure of the acinar lumen appears to play no significant role in determining the rate of saliva secretion.

In short, if one cares only about calculating how much primary saliva is going to be produced, one might as well simply write down an ODE for the apical region of each cell, calculate the fluid flow for each cell independently, and then add them all up.

It is somewhat ironic that we had to construct a multiscale three-dimensional model to show that we didn't need one.

Acknowledgements Since this review appears in a special volume to mark the 90th birthday of Jim Murray, it would be remiss of me (J.S.) not to acknowledge the enormous debt I owe to Jim. Jim has been, for my entire career, an inspiration to me. Not just to me, of course; Jim has been a giant of mathematical biology for decades now, and I am only one of the many who has read, and reread, his book "Mathematical Biology" for both duty and pleasure. It is absolutely fitting that this review, dedicated as it is to a series of results in which it is not always easy to decide whether the modelling stimulated the experiment, or vice versa, appears in a volume dedicated to Jim. I suspect (and hope) he will like this approach, similar as it is to his own. He is, after all, the shoulders I stand on. And, even then, I'm not entirely certain I see any further than he does. This work was supported by NIH Grant 2R01DE019245, and by the Marsden Fund of the Royal Society of New Zealand.

Compliance with Ethical Standards

Conflict of interest The authors declare that they have no conflict of interest.

References

- Almássy J, Won JH, Begenisich TB, Yule DI (2012) Apical Ca^{2+} -activated potassium channels in mouse parotid acinar cells. *J Gen Physiol* 139(2):121–33
- Almássy J, Siguenza E, Skaliczki M, Matesz K, Sneyd J, Yule DI, Nánási PP (2018) New saliva secretion model based on the expression of Na^+ - K^+ pump and K^+ channels in the apical membrane of parotid acinar cells. *Pflugers Arch* 470(4):613–621. <https://doi.org/10.1007/s00424-018-2109-0>
- Ambudkar IS (2012) Polarization of calcium signaling and fluid secretion in salivary gland cells. *Curr Med Chem* 19(34):5774–81
- Ambudkar IS (2014) Ca^{2+} signaling and regulation of fluid secretion in salivary gland acinar cells. *Cell Calcium* 55(6):297–305. <https://doi.org/10.1016/j.ceca.2014.02.009>
- Baum BJ, Zheng C, Cotrim AP, Goldsmith CM, Atkinson JC, Brahim JS, Chiorini JA, Voutetakis A, Leakan RA, Van Waes C, Mitchell JB, Delporte C, Wang S, Kaminsky SM, Illei GG (2006) Transfer of the AQP1 cDNA for the correction of radiation-induced salivary hypofunction. *Biochim Biophys Acta* 1758(8):1071–7. <https://doi.org/10.1016/j.bbamem.2005.11.006>
- Baum BJ, Adriaansen J, Cotrim AP, Goldsmith CM, Perez P, Qi S, Rowzee AM, Zheng C (2010) Gene therapy of salivary diseases. *Methods Mol Biol* 666:3–20. <https://doi.org/10.1007/978-1-60761-820-1>
- Baum BJ, Alevizos I, Chiorini JA, Cotrim AP, Zheng C (2015) Advances in salivary gland gene therapy—oral and systemic implications. *Expert Opin Biol Ther* 15(10):1443–54. <https://doi.org/10.1517/14712598.2015.1064894>
- Baum BJ, Afione S, Chiorini JA, Cotrim AP, Goldsmith CM, Zheng C (2017) Gene therapy of salivary diseases. *Methods Mol Biol* 1537:107–123. <https://doi.org/10.1007/978-1-4939-6685-1>
- Berridge MJ (1990) Calcium oscillations. *J Biol Chem* 265:9583–86
- Berridge MJ (2009) Inositol trisphosphate and calcium signalling mechanisms. *Biochim Biophys Acta* 1793(6):933–40
- Berridge MJ, Galione A (1988) Cytosolic calcium oscillators. *FASEB J* 2:3074–3082
- Berridge MJ, Lipp P, Bootman MD (2000) The versatility and universality of calcium signalling. *Nat Rev Mol Cell Biol* 1(1):11–21
- Cao P, Donovan G, Falcke M, Sneyd J (2013) A stochastic model of calcium puffs based on single-channel data. *Biophys J* 105(5):1133–42. <https://doi.org/10.1016/j.bpj.2013.07.034>
- Chara O, Brusch L (2015) Mathematical modelling of fluid transport and its regulation at multiple scales. *Biosystems* 130:1–10. <https://doi.org/10.1016/j.biosystems.2015.02.004>
- Cook D, Van Lennep E, Mi R, Ja Y (1994) Secretion by the major salivary glands. In: Johnson L (ed) *Physiology of the gastrointestinal tract*, 3rd edn. Raven Press, New York, pp 1061–2017
- Cuthbertson KSR (1989) Intracellular calcium oscillators. In: Goldbeter A (ed) *Cell to cell signalling: from experiments to theoretical models*. Academic Press, London, pp 435–447
- Daniels TE, Wu AJ (2000) Xerostomia—clinical evaluation and treatment in general practice. *J Calif Dent Assoc* 28(12):933–41
- Dawson D (1992) Water transport principles and perspectives. In: Seldin D, Giebisch G (eds) *The kidney physiology and pathophysiology*. Raven Press, New York, pp 301–316
- Diamond JM, Bossert WH (1967) Standing-gradient osmotic flow. A mechanism for coupling of water and solute transport in epithelia. *J Gen Physiol* 50(8):2061–83
- Dolmetsch RE, Xu K, Lewis RS (1998) Calcium oscillations increase the efficiency and specificity of gene expression. *Nature* 392(6679):933–6. <https://doi.org/10.1038/31960>
- Dupont G, Combettes L, Bird GS, Putney JW (2011) Calcium oscillations. *Cold Spring Harb Perspect Biol* 3(3):a004226. <https://doi.org/10.1101/cshperspect.a004226>
- Dupont G, Falcke M, Kirk V, Sneyd J (2016) *Models of calcium signalling, interdisciplinary applied mathematics*, vol 43. Springer, Berlin. <https://doi.org/10.1007/978-3-319-29647-0>
- Ermentrout G, Kopell N (1984) Frequency plateaus in a chain of weakly coupled oscillators. *SIAM J Math Anal* 15:215–37
- Evans RL, Park K, Turner RJ, Watson GE, Nguyen HV, Dennett MR, Hand AR, Flagella M, Shull GE, Melvin JE (2000) Severe impairment of salivation in $\text{Na}^+/\text{K}^+/\text{2Cl}^-$ cotransporter (NKCC1)-deficient mice. *J Biol Chem* 275(35):26720–26726. <https://doi.org/10.1074/jbc.M003753200>
- Fong S, Chiorini JA, Sneyd J, Suresh V (2017) Computational modeling of epithelial fluid and ion transport in the parotid duct after transfection of human aquaporin-1. *Am J Physiol Gastrointest Liver Physiol* 312(2):G153–G163. <https://doi.org/10.1152/ajpgi.00374.2016>

- Foskett JK, Melvin JE (1989) Activation of salivary secretion: coupling of cell volume and $[Ca^{2+}]_i$ in single cells. *Science* 244(4912):1582–5
- Fox RI, Maruyama T (1997) Pathogenesis and treatment of Sjögren's syndrome. *Curr Opin Rheumatol* 9(5):393–9
- Gao R, Yan X, Zheng C, Goldsmith CM, Afione S, Hai B, Xu J, Zhou J, Zhang C, Chiorini JA, Baum BJ, Wang S (2010) AAV2-mediated transfer of the human aquaporin-1 cDNA restores fluid secretion from irradiated miniature pig parotid glands. *Gene Ther* 18(1):38–42
- Garcia GJM, Boucher RC, Elston TC (2013) Biophysical model of ion transport across human respiratory epithelia allows quantification of ion permeabilities. *Biophys J* 104(3):716–26. <https://doi.org/10.1016/j.bpj.2012.12.040>
- Gin E, Crampin EJ, Brown DA, Shuttleworth TJ, Yule DI, Sneyd J (2007) A mathematical model of fluid secretion from a parotid acinar cell. *J Theor Biol* 248(1):64–80
- Gu X, Spitzer NC (1995) Distinct aspects of neuronal differentiation encoded by frequency of spontaneous Ca^{2+} transients. *Nature* 375(6534):784–7. <https://doi.org/10.1038/375784a0>
- Hill AE (2008) Fluid transport: a guide for the perplexed. *J Membr Biol* 223(1):1–11. <https://doi.org/10.1007/s00232-007-9085-1>
- Hong JH, Park S, Shcheynikov N, Muallem S (2014) Mechanism and synergism in epithelial fluid and electrolyte secretion. *Pflugers Arch* 466(8):1487–99. <https://doi.org/10.1007/s00424-013-1390-1>
- Kasai H, Li YX, Miyashita Y (1993) Subcellular distribution of Ca^{2+} release channels underlying Ca^{2+} waves and oscillations in exocrine pancreas. *Cell* 74:669–77
- Keener J, Sneyd J (2008) *Mathematical physiology*, 2nd edn. Springer, New York
- Kopell N, Ermentrout G (1986) Symmetry and phaselocking in chains of weakly coupled oscillators. *Commun Pure Appl Math* 39(5):623–60
- Kopell N, Ermentrout G (1990) Phase transitions and other phenomena in chains of coupled oscillators. *SIAM J Appl Math* 50(4):1014–52
- Kuramoto Y (2003) *Chemical oscillations, waves, and turbulence*. Courier Corporation, New York
- Larsen EH (2002) Analysis of the sodium recirculation theory of solute-coupled water transport in small intestine. *J Physiol* 542(1):33–50
- Larsen EH, Sørensen JB, Sørensen JN (2000) A mathematical model of solute coupled water transport in toad intestine incorporating recirculation of the actively transported solute. *J Gen Physiol* 116(2):101–24. <https://doi.org/10.1085/jgp.116.2.101>
- Layton AT (2011a) A mathematical model of the urine concentrating mechanism in the rat renal medulla. I. Formulation and base-case results. *Am J Physiol Renal Physiol* 300(2):F356–F371. <https://doi.org/10.1152/ajprenal.00203.2010>
- Layton AT (2011b) A mathematical model of the urine concentrating mechanism in the rat renal medulla. II. Functional implications of three-dimensional architecture. *Am J Physiol Renal Physiol* 300(2):F372–F384. <https://doi.org/10.1152/ajprenal.00204.2010>
- Layton AT, Layton HE (2005) A region-based mathematical model of the urine concentrating mechanism in the rat outer medulla. I. Formulation and base-case results. *Am J Physiol Renal Physiol* 289(6):F1346–F1366. <https://doi.org/10.1152/ajprenal.00346.2003>
- Layton AT, Layton HE (2005) A region-based mathematical model of the urine concentrating mechanism in the rat outer medulla. II. Parameter sensitivity and tubular inhomogeneity. *Am J Physiol Renal Physiol* 289(6):F1367–F1381. <https://doi.org/10.1152/ajprenal.00347.2003>
- Lee MG, Xu X, Zeng W, Diaz J, Wojcikiewicz RJ, Kuo TH, Wuytack F, Racymaekers L, Muallem S (1997) Polarized expression of Ca^{2+} channels in pancreatic and salivary gland cells Correlation with initiation and propagation of $[Ca^{2+}]_i$ waves. *J Biol Chem* 272(25):15765–15770
- Lee MG, Ohana E, Park HW, Yang D, Muallem S (2012) Molecular mechanism of pancreatic and salivary gland fluid and HCO_3 secretion. *Physiol Rev* 92(1):39–74. <https://doi.org/10.1152/physrev.00011.2011>
- Li W, Llopis J, Whitney M, Zlokarnik G, Tsien RY (1998) Cell-permeant caged $InsP_3$ ester shows that Ca^{2+} spike frequency can optimize gene expression. *Nature* 392(6679):936–41. <https://doi.org/10.1038/31965>
- Lundberg A (1956) Secretory potentials and secretion in the sublingual gland of the cat. *Nature* 177(4519):1080–1. <https://doi.org/10.1038/1771080a0>
- Lundberg A (1957a) The mechanism of establishment of secretory potentials in sublingual gland cells. *Acta Physiol Scand* 40(1):35–58. <https://doi.org/10.1111/j.1748-1716.1957.tb01476.x>

- Lundberg A (1957b) Secretory potentials in the sublingual gland of the cat. *Acta Physiol Scand* 40(1):21–34. <https://doi.org/10.1111/j.1748-1716.1957.tb01475.x>
- Maclaren OJ, Sneyd J, Crampin EJ (2012) Efficiency of primary saliva secretion: an analysis of parameter dependence in dynamic single-cell and acinus models, with application to aquaporin knockout studies. *J Membr Biol* 245(1):29–50. <https://doi.org/10.1007/s00232-011-9413-3>
- Mangos JA, McSherry NR, Irwin K, Hong R (1973a) Handling of water and electrolytes by rabbit parotid and submaxillary glands. *Am J Physiol* 225(2):450–5. <https://doi.org/10.1152/ajplegacy.1973.225.2.450>
- Mangos JA, McSherry NR, Nousia-Arvanitakis S, Irwin K (1973b) Secretion and transductal fluxes of ions in exocrine glands of the mouse. *Am J Physiol* 225(1):18–24. <https://doi.org/10.1152/ajplegacy.1973.225.1.18>
- Martinez JR (1990) Cellular mechanisms underlying the production of primary secretory fluid in salivary glands. *Crit Rev Oral Biol Med* 1(1):67–78
- Mathias RT, Wang H (2005) Local osmosis and isotonic transport. *J Membr Biol* 208(1):39–53
- Melvin JE (1991) Saliva and dental diseases. *Curr Opin Dent* 1(6):795–801
- Melvin JE (1999) Chloride channels and salivary gland function. *Crit Rev Oral Biol Med* 10(2):199–209
- Melvin JE, Yule D, Shuttleworth T, Begenisich T (2005) Regulation of fluid and electrolyte secretion in salivary gland acinar cells. *Annu Rev Physiol* 67(1):445–469
- Mirollo RE, Strogatz SH (1990) Synchronization of pulse-coupled biological oscillators. *SIAM J Appl Math* 50(6):1645–1662
- Nash MS, Schell MJ, Atkinson PJ, Johnston NR, Nahorski SR, Challiss RAJ (2002) Determinants of metabotropic glutamate receptor-5-mediated Ca^{2+} and inositol 1,4,5-trisphosphate oscillation frequency. Receptor density versus agonist concentration. *J Biol Chem* 277(39):35947–35960. <https://doi.org/10.1074/jbc.M205622200>
- Nathanson MH, Fallon MB, Padfield PJ, Maranto AR (1994) Localization of the type 3 inositol 1,4,5-trisphosphate receptor in the Ca^{2+} wave trigger zone of pancreatic acinar cells. *J Biol Chem* 269(7):4693–6
- Nauntofte B (1992) Regulation of electrolyte and fluid secretion in salivary acinar cells. *Am J Physiol* 263(6 Pt 1):G823–37
- Neu J (1979) Chemical waves and the diffusive coupling of limit cycle oscillators. *SIAM J Appl Math* 36:509–515
- Novotny JA, Jakobsson E (1996a) Computational studies of ion-water flux coupling in the airway epithelium. I. Construction of model. *Am J Physiol* 270(6 Pt 1):C1751–C1763
- Novotny JA, Jakobsson E (1996b) Computational studies of ion-water flux coupling in the airway epithelium. II. Role of specific transport mechanisms. *Am J Physiol* 270(6 Pt 1):C1764–C1772
- Pages N, Vera-Sigüenza E, Rugis J, Kirk V, Yule DI, Sneyd J (2019) A model of Ca^{2+} dynamics in an accurate reconstruction of parotid acinar cells. *Bull Math Biol* 81(5):1394–1426. <https://doi.org/10.1007/s11538-018-00563-z>
- Palk L, Sneyd J, Shuttleworth TJ, Yule DI, Crampin EJ (2010) A dynamic model of saliva secretion. *J Theor Biol* 266(4):625–40
- Palk L, Sneyd J, Patterson K, Shuttleworth TJ, Yule DI, Maclaren O, Crampin EJ (2012) Modelling the effects of calcium waves and oscillations on saliva secretion. *J Theor Biol* 305:45–53
- Patterson K, Catalán MA, Melvin JE, Yule DI, Crampin EJ, Sneyd J (2012) A quantitative analysis of electrolyte exchange in the salivary duct. *Am J Physiol Gastrointest Liver Physiol* 303(10):G1153–63. <https://doi.org/10.1152/ajpgi.00364.2011>
- Peña-Münzenmayer G, Catalán MA, Kondo Y, Jaramillo Y, Liu F, Shull GE, Melvin JE (2015) Ae4 (Slc4a9) anion exchanger drives Cl⁻ uptake-dependent fluid secretion by mouse submandibular gland acinar cells. *J Biol Chem* 290(17):10677–10688. <https://doi.org/10.1074/jbc.M114.612895>
- Reuss L (2002) Water transport controversies—an overview. *J Physiol* 542(1):1–2
- Sandefur CI, Boucher RC, Elston TC (2017) Mathematical model reveals role of nucleotide signaling in airway surface liquid homeostasis and its dysregulation in cystic fibrosis. *Proc Natl Acad Sci USA* 114(35):E7272–E7281. <https://doi.org/10.1073/pnas.1617383114>
- Ship JA, Fox PC, Baum BJ (1991) How much saliva is enough? “Normal” function defined. *J Am Dent Assoc* 122(3):63–9
- Siekman I, Wagner LE, Yule D, Crampin EJ, Sneyd J (2012) A kinetic model for type I and II IP₃R accounting for mode changes. *Biophys J* 103(4):658–68

- Silva P, Stoff J, Field M, Fine L, Forrest JN, Epstein FH (1977) Mechanism of active chloride secretion by shark rectal gland: role of Na-K-ATPase in chloride transport. *Am J Physiol* 233(4):F298–306. <https://doi.org/10.1152/ajprenal.1977.233.4.F298>
- Sneyd J, Tsaneva-Atanasova K, Bruce JIE, Straub SV, Giovannucci DR, Yule DI (2003) A model of calcium waves in pancreatic and parotid acinar cells. *Biophys J* 85(3):1392–405. [https://doi.org/10.1016/S0006-3495\(03\)74572-X](https://doi.org/10.1016/S0006-3495(03)74572-X)
- Sneyd J, Tsaneva-Atanasova K, Reznikov V, Bai Y, Sanderson MJ, Yule DI (2006) A method for determining the dependence of calcium oscillations on inositol trisphosphate oscillations. *Proc Natl Acad Sci USA* 103(6):1675–80. <https://doi.org/10.1073/pnas.0506135103>
- Sneyd J, Crampin E, Yule D (2014) Multiscale modelling of saliva secretion. *Math Biosci* 257:69–79. <https://doi.org/10.1016/j.mbs.2014.06.017>
- Sneyd J, Han JM, Wang L, Chen J, Yang X, Tanimura A, Sanderson MJ, Kirk V, Yule DI (2017) On the dynamical structure of calcium oscillations. *Proc Natl Acad Sci USA* 114(7):1456–1461. <https://doi.org/10.1073/pnas.1614613114>
- Swanson CH (1977) Isotonic water transport in secretory epithelia. *Yale J Biol Med* 50(2):153–63
- Thorn P (1996) Spatial domains of Ca^{2+} signaling in secretory epithelial cells. *Cell Calcium* 20:203–214
- Thorn P, Lawrie AM, Smith PM, Gallacher DV, Petersen OH (1993) Local and global cytosolic Ca^{2+} oscillations in exocrine cells evoked by agonists and inositol trisphosphate. *Cell* 74(4):661–8
- Thul R, Bellamy TC, Roderick HL, Bootman MD, Coombes S (2008) Calcium oscillations. *Adv Exp Med Biol* 641:1–27
- Torre V (1975) Synchronization of non-linear biochemical oscillators coupled by diffusion. *Biol Cybern* 17:137–144
- Tosteson D, Hoffman J (1960) Regulation of cell volume by active cation transport in high and low potassium sheep red cells. *J Gen Physiol* 44:169–94
- Turner RJ, Sugiya H (2002) Understanding salivary fluid and protein secretion. *Oral Dis* 8(1):3–11
- Vera-Sigüenza E, Catalán MA, Peña-Münzenmayer G, Melvin JE, Sneyd J (2018) A mathematical model supports a key role for Ae4 (Slc4a9) in salivary gland secretion. *Bull Math Biol* 80(2):255–282. <https://doi.org/10.1007/s11538-017-0370-6>
- Vera-Sigüenza E, Pages N, Rugis J, Yule DI, Sneyd J (2019) A mathematical model of fluid transport in an accurate reconstruction of parotid acinar cells. *Bull Math Biol* 81(3):699–721. <https://doi.org/10.1007/s11538-018-0534-z>
- Vera-Sigüenza E, Pages N, Rugis J, Yule DI, Sneyd J (2020) A multicellular model of primary saliva secretion in the parotid gland. *Bull Math Biol* 82(3):38. <https://doi.org/10.1007/s11538-020-00712-3>
- Warren NJ, Tawhai MH, Crampin EJ (2009) A mathematical model of calcium-induced fluid secretion in airway epithelium. *J Theor Biol* 259(4):837–849
- Watt SD, Gu X, Smith RD, Spitzer NC (2000) Specific frequencies of spontaneous Ca^{2+} transients upregulate GAD 67 transcripts in embryonic spinal neurons. *Mol Cell Neurosci* 16(4):376–87. <https://doi.org/10.1006/mcne.2000.0871>
- Weinstein A (1994) Mathematical models of tubular transport. *Ann Rev Physiol* 56:691–709
- Weinstein AM (1999) Modeling epithelial cell homeostasis: steady-state analysis. *Bull Math Biol* 61(6):1065–1091
- Weinstein AM (2020) A mathematical model of the rat kidney. *Antidiuresis. Am J Physiol Renal Physiol* II. <https://doi.org/10.1152/ajprenal.00046.2020>
- Weinstein AM, Stephenson JL (1979) Electrolyte transport across a simple epithelium. Steady-state and transient analysis. *Biophys J* 27(2):165–86. [https://doi.org/10.1016/S0006-3495\(79\)85209-1](https://doi.org/10.1016/S0006-3495(79)85209-1)
- Weinstein AM, Stephenson JL (1981a) Coupled water transport in standing gradient models of the lateral intercellular space. *Biophys J* 35(1):167–191
- Weinstein AM, Stephenson JL (1981b) Models of coupled salt and water transport across leaky epithelia. *J Membr Biol* 60(1):1–20
- Wu D, Boucher RC, Button B, Elston T, Lin CL (2018) An integrated mathematical epithelial cell model for airway surface liquid regulation by mechanical forces. *J Theor Biol* 438:34–45. <https://doi.org/10.1016/j.jtbi.2017.11.010>